

## COEFFICIENT OF FRICTION AT REST OF ROUGH SURFACES

Khairaliyev S.<sup>1\*</sup>, Kaishubayeva N.<sup>2</sup>, Kapayeva S.<sup>3</sup>, Bergander Marek J.<sup>4</sup>, Dzhundibayev V.<sup>5</sup>

<sup>1</sup> Intekko Ltd, Astana, Kazakhstan, kh.serik@gmail.com

<sup>2</sup> Rauza-PV LLP, Astana, Kazakhstan

<sup>3</sup> East-Kazakh Technical University, Ust-Kamenogorsk, Kazakhstan

<sup>4</sup> Magnetic Development INC., Madison, USA

<sup>5</sup> L.N. Gumilyov Eurasian National University, Astana, Kazakhstan

*At present, the process of designing dry friction units for mechanical engineering and some other structures is becoming more and more laborious, forcing designers to make more and more efforts in this work. A significant complication of the work performed gives the random nature of the roughness of both contacting surfaces and this circumstance forces the designers to look for new ways to solve existing problems. In this paper, we consider the contact interaction of two rough parts, the roughness of which is modeled by spherical surfaces. The proposed friction pair model makes it possible to estimate the interaction forces of contacting rough surfaces acting between the considered surfaces. It should be emphasized that this paper considers the interaction of contacting bodies with an applied external force capable of starting the relative movement / sliding of the considered bodies with rough surfaces.*

**Keywords:** Rough surface; analytical modelling; static interaction of rough surfaces

### Introduction

Descriptions of the various friction phenomena was attempted in numerous studies by considering the surface roughness effect. Surface topography observed in microscopic scale was proved to be extremely rough and of random nature, composed of alternating ledges and hollows of various dimensions referred to as surface heights, or asperities and micro cavities. One of the earliest models to describe surface roughness was presented by Archard. It represented the rough surfaces as spherical asperities consisting of smaller asperities in recursion, which would deform elastically at the points of contact with another surface [1]. The true area of contact then would be the summation of the areas of contact of each of the asperities [1].

On the other hand, Zhuravlev modeled roughness as spherical irregularities of the same size, located at different heights with a linear distribution [2]. Based on the Hertz solution for two contacting rough surfaces, it was concluded that the true contact area is proportional to the normal load [2]. Archard's and Zhuravlev's models were further developed by Greenwood and Williamson to incorporate Gaussian distribution of asperity heights and plastic deformation of asperities beyond the elasticity limit [3]. They showed that whether the asperities deform elastically or plastically did not depend on the normal load, and as an indication of the type of deformation plasticity index,  $\psi$ , was introduced.

Later Bush, Gibson and Thomas proposed a model (BGT model) of roughness as elastically deformed paraboloids distributed according to the random process model [4]. On the other hand, Kragelsky et al. [5] modelled roughness as elastic rods of varying heights. The authors' equation for the function of the normal force,  $N$ , with respect to rough planes' separation,  $a$ , revealed that the contact area,  $A_c$ , had linear dependence on normal load [4].

Numerical modelling is also used to describe the roughness and analyze the friction. For example, Ogilvy [6] produced a numerical model of statistically distributed elastic and plastic asperities, and estimated the friction coefficients through the adhesive force (microscale) and the overall true area of contact (macroscale). On the other hand, Karpenko and Akay [7] did computational three-dimensional modelling of elastic deformations. Ford also numerically estimated the effect of contact angle in the Greenwood and Williamson's model for elastic and plastic deformation [3]. These deformations were also addressed in [8] taking into account the control volume conservation. Statistical calculations were also performed for microslip [9] and fretting phenomena [10]. Serious works include the book by Kragelsky [11] and the book written

under the direction of Chichinadze [12]. In these books, the geometric parameters of rough friction surfaces are considered in detail and the processes of their contact interaction are modeled.

The contact of surfaces was considered in [13] with spherical roughness in the absence of an external horizontal force. The performed calculations made it possible to come to the conclusion about the reasonableness of using the model considered here for calculating the forces of contact interaction.

## 1 Friction force model

The main goal of this work is to calculate the static friction force, for which the model of a friction pair was adopted, the initial consideration of which was carried out in [13]. To calculate the forces of contact interaction, we use the model shown in Fig. 1. It is quite obvious that in real conditions not all irregularities of the contacting parts of the friction unit are in contact with each other and the calculation will be performed in this way - the most realistic case will be taken into consideration when only a part of the roughness of both parts are in contact.

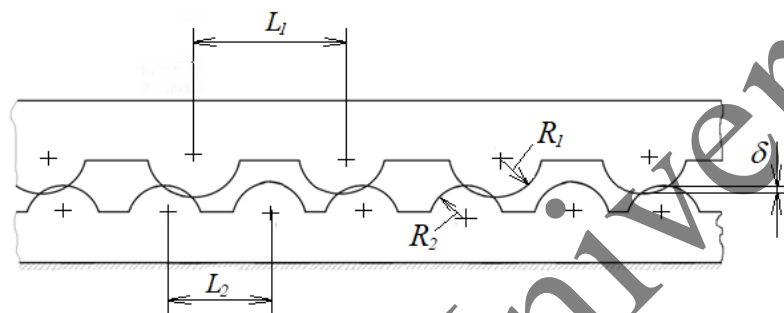


**Fig1.** Two rough contact surfaces (the slider and the base):

$R_1$  and  $R_2$  are micro-roughness radii of the slider and the base, respectively,  $\delta$  is the overlapping of the pair of contacting micro-asperities in the vertical direction,  $L_1$  and  $L_2$  are period of micro-roughness of the slider and the base.

The contact of the roughness of the slide and the roughness of the base is shown in Fig. 2, the irregularities shown here are interacting. The vertical force and the horizontal force are shown in Fig. 2 and we will consider how these forces can be determined. Obviously, the sum / integral of all vertical forces in each contact must be equal to the external vertical force and the sum / integral of all horizontal forces in each contact must be equal to the external horizontal force.

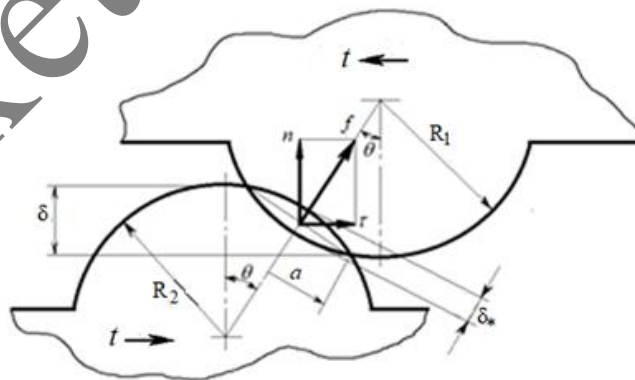


**Fig. 2.** Mechanical contact model between two asperities:

$f$  is the contact reaction along the line connecting the centers of the radii of the slide and the base,  $n$  and  $\tau$  are the vertical and the horizontal forces of interaction in the normal and horizontal directions,  $a$  is the radius of the contact circle of microroughness,  $\theta$  is the angle between the vertical line and the line connecting the centers.  $t$  is that part of the external force that acts on the considered roughness.

Different authors approach the calculation of the friction force with different bases [11]:

- friction is explained by lifting along microroughness;
- friction is explained as the result of overcoming the forces of molecular interaction between two solids;
- friction arises as a deformation force;
- a combined approach to determining the friction force.

In this work, the forces of interaction arising from the contact of spherical roughness will be determined. During friction of rough surfaces, a rather large number of pairs of roughness come into contact, as in Fig. 2; all contacting pairs of roughness are at different angle  $\theta$ . For further consideration of a real friction pair, a model will be adopted in which all contacting spheres of the base are reduced to one protrusion (part of the sphere) in Fig. 3, and the contacting protrusions of the slider, i.e. undoubtedly in different positions in relation to the base are shown in Fig. 3 as a deformable medium (here it looks like a gray mass).

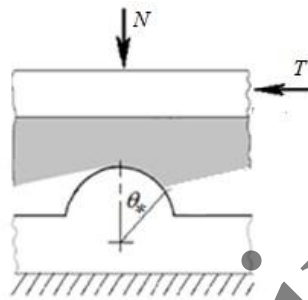


**Fig. 3.** Contact of the roughness of the slide, reduced to one roughness of the base.  $\theta_*$  is the initial contact angle.

We consider the moment of the beginning of contact, Fig. 3 is shown somewhat simplified for such a position - in the left part of the upper body, the material allegedly "does not have time" to return to the "undeformed state", but in fact the left part of the body does not deform and the figure shows it in such a way that the process under consideration was clearer. Consider the case when an external horizontal force  $T$  is applied to the slider on the right-side, forcing the slider to move to the left. For the slider to start sliding on the base, the magnitude of this force must reach a certain value, which is classified as the static friction force. It is quite reasonable to assume that at the moment of the beginning of sliding, the contact forces between the roughness of the slider and the base in the left half of the roughness of the base become equal to zero.

The primary consideration of the forces of contact interaction of the slider with the base without the application of an external horizontal force  $T$  was carried out in [13]. Now we must calculate the horizontal force  $T$ , and also take into account the fact that the contact of the roughness of the slider and the base occurs as shown in Fig. 3. In [13], the following formulas were derived for calculating the contact forces of the roughness of the slide and the base

$$n = c_\theta (\theta_*^2 - \theta^2)^{3/2}; \tag{1}$$

$$\tau = c_\theta \theta (\theta_*^2 - \theta^2)^{3/2}, \tag{2}$$

where  $\theta_*$  is the angle at which the beginning of contact between the roughness of the slider and the base is possible ( $\theta_0$  has the same definition, but it is used in the absence of horizontal forces including friction forces as shown in Fig.3); the following values were also taken in [13] for calculations:

$$c_\theta = c \left( \frac{R_1 + R_2}{2} \right)^{3/2}; \quad c = \frac{4}{3} R^{1/2} E,$$

and

$$\frac{1}{R} = \frac{1}{R_1} + \frac{1}{R_2} \quad R = \frac{R_1 R_2}{R_1 + R_2}, \quad E = \frac{E_1 E_2}{E_1 (1 - \mu_1^2) + E_2 (1 - \mu_2^2)}.$$

(1) and (2) describe the  $\mu_l$  forces of interaction in a single contact. The total force of interaction of friction surfaces can be found by summing / integrating all contacts of the roughness of the slide and the base. The vertical and horizontal forces of contact of friction surfaces are:

$$N = \frac{j_a c \theta}{2\theta_L} \int_0^{\theta_*} (\theta_*^2 - \theta^2)^{3/2} d\theta. \quad (1)$$

$$T = \frac{j_a c \theta}{2\theta_L} \int_0^{\theta_*} (\theta_*^2 - \theta^2)^{3/2} \theta d\theta. \quad (4)$$

Here  $\theta_L = \frac{L_1 + L_2}{2(R_1 + R_2)}$  is the greatest angle up to which it is assumed that the micro-asperity of the slider is opposed to the micro-asperity of the base,  $j_a$  is the number of contacting pairs of roughness in the contact zone; the calculations will use the value of the change  $\Delta j_a$  with an increase in the vertical force  $N$  and the approach of the friction surfaces under the action of an external normal force.

In the future, we will carry out calculations with the assumptions that as the slide and the base come closer under the action of an external force, the number of contacting pairs of roughness increases. The stiffness of the roughness of the slider and the base, which come into contact with an increase in the normal force and the approach of the contacting bodies, undoubtedly differs in magnitude from the stiffness of the roughness that came into contact before the considered moment. However, in the proposed primary consideration of the contacting surfaces, we will assume that the rigidity of all contacting pairs of roughness is the same.

As can be seen, in equations (3) and (4) the integral is taken within the limits different from the limits used in [13] - here it is taken from zero to  $\theta_*$  on the side where the contact begins and, as can be seen, after passing the vertex roughness contact disappears. As a result of integrating formulas (3) and (4), we obtain the following expressions for calculating the normal force and horizontal (frictional) force

$$N = \frac{3\pi j_a c \theta_*^4}{32\theta_L} \quad (5)$$

$$T = \frac{j_a c \theta_*^5}{10\theta_L} \quad (6)$$

The coefficient of friction now can be calculated

$$\mu = \frac{T}{N} \quad (7)$$

The used model of two contacting bodies with a rough surface makes it possible to trace the process of the formation of the friction force at relative rest of the contacting bodies and to simulate the process of friction of rough surfaces. In our opinion, the considered model also makes it possible to explain the main reasons for the increase and decrease in the coefficient of friction. We believe that the theoretical calculation of the friction force performed in Section 2 makes sense and gives a good idea of the dependence of the friction coefficient on the normal force.

## 2 Results and discussion

Based on the experience of our work, we want to say that as the vertical external force increases, the slider and the base approach each other and, at the same time, the number of pairs of new microasperities entering into contact decreases. Nevertheless, we believe it is possible to perform the initial calculation of the process of increasing the external force with a constant number of pairs of roughnesses coming into contact, but this can only be done at the initial stage of modeling a contacting friction pair. Further, on the basis of the formulas presented here, graphs of the dependence of the friction coefficient on the values characterizing the considered friction pair are constructed.

**Table 1.** Common parameters for all systems shown in the following graphs

$R_1, m$	$R_2, m$	$L_1, m$	$L_2, m$	$E_1, Pa$	$\mu_1$	$E_2, Pa$	$\mu_2$
$1.5 \cdot 10^{-5}$	$2.0 \cdot 10^{-5}$	$1.6 \cdot 10^{-4}$	$2.0 \cdot 10^{-4}$	2.2000E+11	0.25	2.2000E+11	0.25

Fig. 4 shows three graphs of the dependence of the coefficient of friction of materials with the characteristics indicated in Table 1, and the radii of roughness and the number of these roughness are given in Table 2. It can be seen that with an increase in the normal force  $N$  applied to the friction pair, the coefficient  $\mu$  of static friction increases.

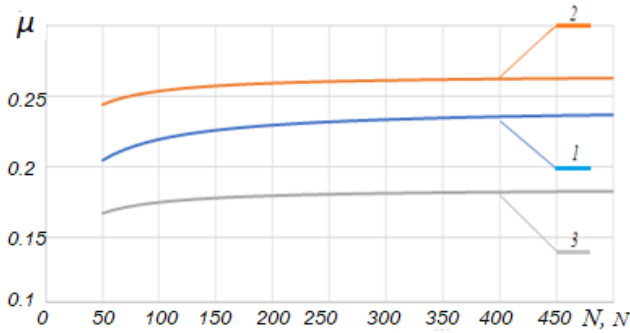


**Table 2.** The parameters of the graphs in Fig.4.

	1	2	3
$j_a$	10	7	15
$\Delta j_a$	1	1	2

**Fig. 4.** The dependence of the coefficient of friction  $\mu$  on the pressing force (all values are in table 2).

Earlier it was said that the change in the number of contacting roughness  $\Delta j_a$  occurs with an increase in the vertical force  $N$ . It would be more correct to specify the change in the number of roughness depending on the increase in the depth of immersion of the slider roughness in the roughness of the base, but in this first work it is assumed in a simplified way that the number contacting roughness increases depending on the applied vertical force  $N$ .

Fig. 4 shows graphs of the coefficient of friction for three different friction surfaces. The curve constructed for friction pair 2 has the least roughness and, in our opinion, with a smaller number of roughness, the slider penetrates deeper into the roughness of the base and this creates a greater value of the friction coefficient. The friction pair, for which curve 3 is constructed, has a large number of roughness and this leads to less convergence of the bodies and a lower coefficient of friction. Friction pair number 1 has an average number of roughness and creates an average value of the friction coefficient.

On Fig. 5 graphs are constructed for materials with the same roughness parameters (radii) as those considered in Fig. 4, but the amount of roughness is different. It can be seen that in Fig. 4, the initial number of roughness is greater than in Fig. 5, but the subsequent increase in the number of contacting roughness is less than that shown in Figs. 5. As can be seen, a large initial number of roughness and their slight increase with an increase in the vertical force pressing the slider to the base leads to an increase in the friction coefficient with an increase in the vertical force pressing the slider.

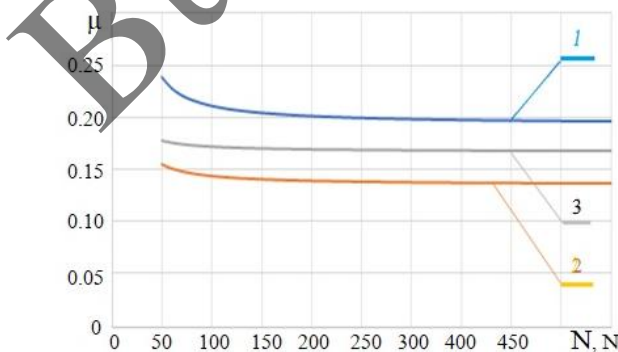


**Table 3.** The parameters of the graphs in Fig. 5.

	1	2	3
$j_a$	5	10	8
$\Delta j_a$	2	3	2

**Fig. 5.** The dependence of the coefficient of friction  $\mu$  on the pressing force (all values are in table 3).

In the case of a smaller initial number of roughnesses and with a larger number of roughnesses that come into contact with an increase in the vertical external force, the friction coefficient decreases with an increase in the external vertical force. As becomes obvious, with a larger number of microroughnesses, the friction coefficient decreases. Why? With a larger number of roughnesses, each contacting pair has a smaller contact force and this leads to the fact that the contact angle is smaller, the contact roughnesses of both friction pairs are in contact at a smaller angle (closer to their top).

Fig. 6 shows three graphs with the same parameters at the initial moment of contact, but with a subsequent increase in force, the number of microroughnesses that come into contact again differs. The deformation turns out to be greater for the friction pair, in which the number of roughnesses is less, and if the friction pair has more microroughnesses, the friction coefficient is lower.

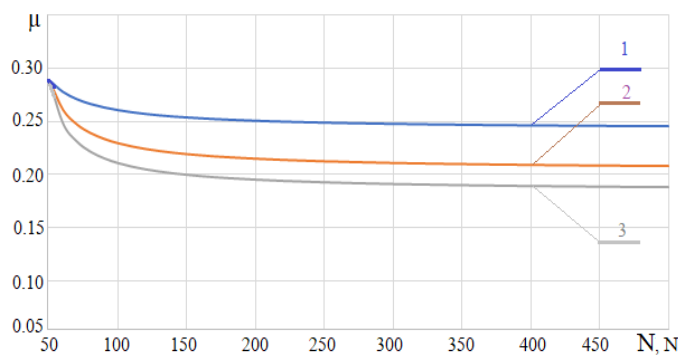


**Fig. 6.** The dependence of the coefficient of friction  $\mu$  on the pressing force (all values are in table 4).

**Table 4.** The parameters of the graphs in Fig. 6.

	1	2	3
$j_a$	5	5	5
$\Delta j_a$	2	4	6

Thus, the chosen model of two contacting bodies with a rough surface makes it possible to trace the process of the formation of the friction force at relative rest of the bodies under consideration and, in our opinion, makes it possible to explain the main reasons for the increase and decrease in the coefficient of friction. The graphs in Fig. 7 turned out to be interesting. As can be seen from Table 5, the radii of curvature of the roughness of all three surfaces are the same, only the number of roughness differs, but an increase in the number of roughness occurs with the same ratio  $j_a / \Delta j_a = 5$  with an increase in the external force by 10 N.

As can be seen in Fig. 7, while all three graphs of the friction coefficients remain constant - they do not change at any value of the vertical force. It should be said that we obtained the same effect with the same ratio ( $j_a / \Delta j_a = 5$ ) in other systems with other values of the roughness radii. Apparently, it is worth pondering over this phenomenon and finding out how real the effect obtained here is.

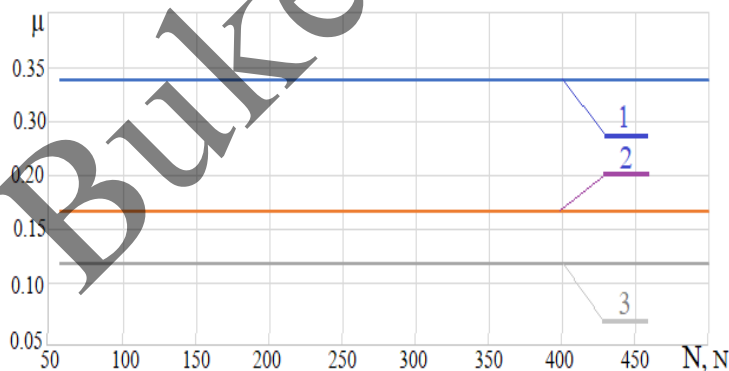


**Fig. 7.** The dependence of the coefficient of friction  $\mu$  on the pressing force (all values are in table 5).

**Table 5.** The parameters of the graphs in Fig. 7.

	1	2	3
$j_a$	5	5	5
$\Delta j_a$	2	4	6

We find another graph of the dependence of the coefficient of friction on the force useful. On Fig. 8 four graphs of the dependence of the coefficient of friction on the number of microroughnesses are shown; we are ready to say once again that not all the graphs shown in this paper can be found in real friction pairs, but they allow us to understand the law of formation of the friction force.

Fig. 8 shows four graphs of the dependence of the coefficient of friction on the pressing force of the friction bodies. As can be seen, the fourth friction pair has the largest initial number of microroughnesses (this is unlikely), but the subsequent number of microroughnesses grows absolutely the same for all four friction pairs. The second friction pair seems to be the most realistic, because the friction coefficient shows the most frequently occurring values. It is possible to see the first and third pairs of friction in real life, but not very often; the fourth pair seems quite unrealistic.

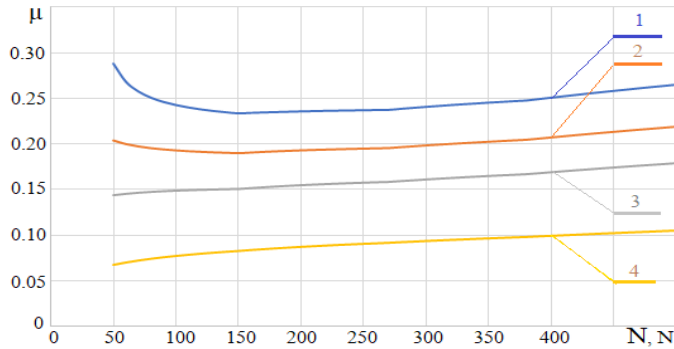


**Table 6.** The parameters of the graphs in Fig. 8.

	$j_a$	$\Delta j_a$
1	5	3210
2	10	3210
3	20	3210
4	90	3210

**Fig. 8.** The dependence of the coefficient of friction  $\mu$  on the pressing force with different number of microroughness.

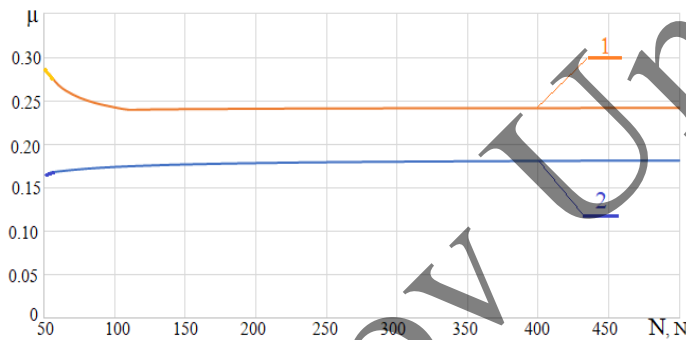


**Table 7.** The parameters of the graphs in Fig. 9.

	$j_a$	$\Delta j_a$
1	5	3210
2	15	2310

**Fig. 9.** The dependence of the coefficient of friction  $\mu$  on the pressing force with different number of microroughness.

As can be seen in Fig. 9, the coefficient of friction of material 1 first decreases and then very slowly increases. Material 2 grows noticeably at first, but then grows very slowly (outwardly, the graph looks almost unchanged). We have chosen to include these two graphs because they seem to be quite typical and have not yet included other friction pairs in this article, since the friction model requires understanding of real contact processes.

### Conclusion

We modeled many friction pairs and chose for this article those that exhibit the most characteristic and understandable friction properties, and added several other friction pairs that seem unlikely, but show quite interesting properties. This article examines the static contact of rough surfaces under the action of normal and shear (horizontal) forces on them, the action of which is resisted by the static friction force. When solving such a problem, the surface roughness is represented by spherical protrusions, the parameters of which are the same within one surface. The results obtained as a result of solving these problems allow us to consider the reaction of rubbing bodies for different characteristics of rough surfaces.

---

---

## References

- 1 Archard J.F. Elastic Deformation and the Laws of Friction. *Proceedings of the Royal Society of London*, 1957, Vol. 243, pp. 190–205. doi: 10.1098/rspa.1957.0214
- 2 Zhuravlev V.A. On the question of theoretical justification of the Amontons-Coulomb law for friction of unlubricated surfaces. *Proceedings of the Institution of Mechanical Engineers, Part J - Journal of Engineering Tribology*. 2007, No. 221, pp. 893-895. doi: 10.1243/13506501JET176
- 3 Greenwood J.A., Williamson J.B.P. Contact of Nominally Flat Surfaces. *Proceedings of the Royal Society of London A*, 1966, Is. 295(1442), pp. 300–319. doi: 10.1098/rspa.1966.0242
- 4 Bush A.W., Gibson R.D., Thomas T.R. The elastic contact of a rough surface. *Wear*, 1975, 35(1), pp. 87–111. doi: 10.1016/0043-1648(75)90145-3
- 5 Kragelskii I.V., Dobychin M.N., Kombatov V.S. *Friction and Wear. Calculation methods*. Oxford: Pergamon Press Ltd. 474 p. eBook. Available at: <https://shop.elsevier.com/books/friction-and-wear/kragelsky/978-0-08-025461-6>
- 6 Ogilvy J.A. Numerical simulation of friction between contacting rough surfaces. *J. Phys. D. Appl. Phys.*, 1991, No. 24(11), pp. 2098–2109. doi: 10.1088/0022-3727/24/11/030
- 7 Karpenko Y.A., Akay A.A numerical model of friction between rough surfaces. *Tribol. Int.*, 2001, No.34(8), pp. 531–545. doi: 10.1016/S0301-679X(01)00044-5
- 8 Chang W.R., Etsion I., Bogy D.B. An Elastic-Plastic Model for the Contact of Rough Surface. *J. Tribol.*, 1987, No. 109(2), pp. 257–263. doi: 10.1115/1.3261348
- 9 Bjorklund S.A random model for micro-slip between nominally flat surfaces. *J. Tribol.*, 1997, 119(4), pp. 726–732. doi: 10.1115/1.2833877
- 10 Eriten M., Polycarpou A.A., BergmaL.A. Physics-based modeling for fretting behavior of nominally flat rough surfaces. *Int. J. Solids Struct.*, 2011, 48(10), pp. 1436–1450. doi: 10.1016/j.ijsolstr.2011.01.028
- 11 Kragelskii I.V. *Friction and Wear*. Elmsford: Pergamon Press, 1982, 420 p.
- 12 Chichinadze A.V., Braun E.D., Bushe N.A., et al. *Fundamentals of Tribology. Friction, Wear, and Lubrication*. Moscow, Mashinostroyeniye Publ., 2001. 664 p. [in Russian]
- 13 Khairaliyev S.I., Kaishubayeva N., Spitas Ch., Dzhundibayev V. Static interaction of rough surfaces under normal force. *Eurasian Physical Technical Journal*, 2020, Vol.17, No.2(34), pp.110-115. doi 10.31489/2020No2/110-115.